Effect of local soil conditions on the seismic response of free-standing multi-drum ancient Greek columns

S. Karafagka[1], and K. Pitilakis[2]

[1]*Asst. Professor, Department of Civil Engineering, University of the Peloponnese, Patras, Greece, email: s.karafagka@uop.gr*

[2]*Emeritus Professor, Department of Civil Engineering, Aristotle University of Thessaloniki, Greece, email: kpitilak@civil.auth.gr*

ABSTRACT

Ancient Greek temples are not always founded on rock; thus, the seismic response of free-standing multi-drum columns may be significantly influenced by soil deformability. Foundation compliance alters the excitation transmitted to the structure and governs rocking and permanent deformations. Despite its importance, the role of local soil conditions in the seismic behaviour of such systems remains insufficiently explored. This preliminary study of the response of a representative multi-drum column founded on soft soil deposits aims to offer an initial insight into how its performance may be affected. Three single-layer sand profiles corresponding to Eurocode 8 soil classes B, C and D are analysed and compared with a fixed-base (Class A) reference configuration. Three-dimensional nonlinear dynamic time-history analyses are performed, modelling the drums as deformable blocks interacting through frictional contact, while the soil is represented as an elasto–plastic continuum with absorbing boundaries to simulate radiation damping and soil–structure interaction effects. The seismic response is evaluated through engineering demand parameters describing peak rocking demand, cycle-by-cycle motion, and residual displacements, capturing both transient and cumulative behaviour. Results show that soil deformability substantially modifies the column kinematics, affecting not only peak displacements but also the accumulation of residual deformations. The response does not vary monotonically with soil stiffness, highlighting the complex interplay between foundation compliance, excitation characteristics, and rocking dynamics. These findings emphasise that soil–structure interaction governs the seismic performance of multi-drum columns on medium-stiff to soft soils and should be explicitly considered in their assessment and conservation.

Keywords: Ancient multi-drum column, Soil-structure interaction, Rocking/Sliding phenomena, Nonlinear seismic response, Abaqus dynamic analysis, Soil class effects

INTRODUCTION

Archaeological and geotechnical evidence indicates that many ancient Greek columns and temples were founded on deformable or heterogeneous ground conditions rather than on rigid bedrock. Soft alluvial deposits, constructed fills and variable foundation soils have been documented at emblematic sites such as the Ancient Agora of Athens (Thompson, 1953), the Heraion of Samos, the Temple of Artemis at Ephesus, and the sanctuaries of Didyma and Olympia (Tsatsanifos, 2023). These observations suggest that soil–structure interaction (SSI) was not an exceptional condition, but rather an inherent feature of the seismic environment of ancient monuments.

In the presence of deformable foundation soils, the seismic response of free-standing multi-drum columns is governed not only by the mechanics of rocking and sliding at the drum interfaces (Konstantinidis & Makris, 2005), but also by the dynamic interaction between the structure and the supporting ground. Foundation compliance alters the characteristics of the seismic motion transmitted to the column and modifies the kinematics of the rocking response through soil deformability, radiation damping and potential soil yielding. These effects influence the initiation of rocking, the amplitude and persistence of oscillations, and the accumulation of permanent deformations. Consequently, the seismic performance of columns founded on deformable soil cannot be reliably inferred from fixed-base (bedrock) analyses alone.

Recent studies on historical and monumental structures have demonstrated that soil conditions and SSI can substantially affect natural periods, rocking thresholds and overall seismic vulnerability (Karatzetzou et al., 2021; Amendola & D. Pitilakis, 2022; Marinos et al., 2025). However, most existing analyses rely primarily on global response measures or peak deformation indices, which are insufficient to capture the full kinematic evolution of multi-drum systems when the foundation is not effectively rigid. In particular, the relative and cumulative displacements between drums, as well as the progressive loss of re-centring capacity, are strongly controlled by soil deformability and are not adequately described by peak response alone (Stiros, 2020).

Motivated by this gap, the present study focuses explicitly on the influence of foundation soil conditions on the seismic response of a representative free-standing multi-drum column. Three single-layer sand profiles representative of Eurocode 8 soil classes B, C and D are examined and compared with a fixed-base configuration representing bedrock conditions (Class A). Fully nonlinear three-dimensional dynamic time-history analyses are performed in Abaqus (Dassault Systèmes, 2022), explicitly accounting for rocking, sliding and separation at the drum interfaces, as well as soil–structure interaction effects. The objective is not only to quantify changes in peak displacement demand, but also to investigate how soil deformability governs the evolution of cyclic motion, cumulative drift and permanent deformation. By employing both global and cycle-based engineering demand parameters, the study aims to provide a first order physically consistent interpretation of the seismic response of free-standing multi-drum columns on deformable soils, highlighting the mechanisms through which foundation conditions influence stability and global earthquake performance.

NUMERICAL MODELLING

Structural Modelling of the Multi-Drum Column

The free-standing multi-drum column is modelled as a fully three-dimensional (3D) structure using the finite element code Abaqus. A fully 3D formulation is essential, since two-dimensional idealisations may underestimate rocking and sliding effects and artificially increase the predicted seismic stability (Psycharis, 2014). The column replicates the geometry of a typical Parthenon Doric column, consisting of eleven cylindrical drums and a capital, with a total height of 10.44 m and a slenderness ratio of approximately 5.80 (Figure 1a-b). Each drum is represented as a deformable solid using eight-node linear brick elements available in Abaqus (C3D8), with geometric nonlinearity activated to allow for large rotations, uplift, separation and re-contact during seismic excitation. The mesh density was selected based on a sensitivity analysis ensuring accurate representation of the nonlinear rocking response without excessive computational cost, in line with established recommendations for modelling ancient multi-drum structures (K. Pitilakis et al., 2017).

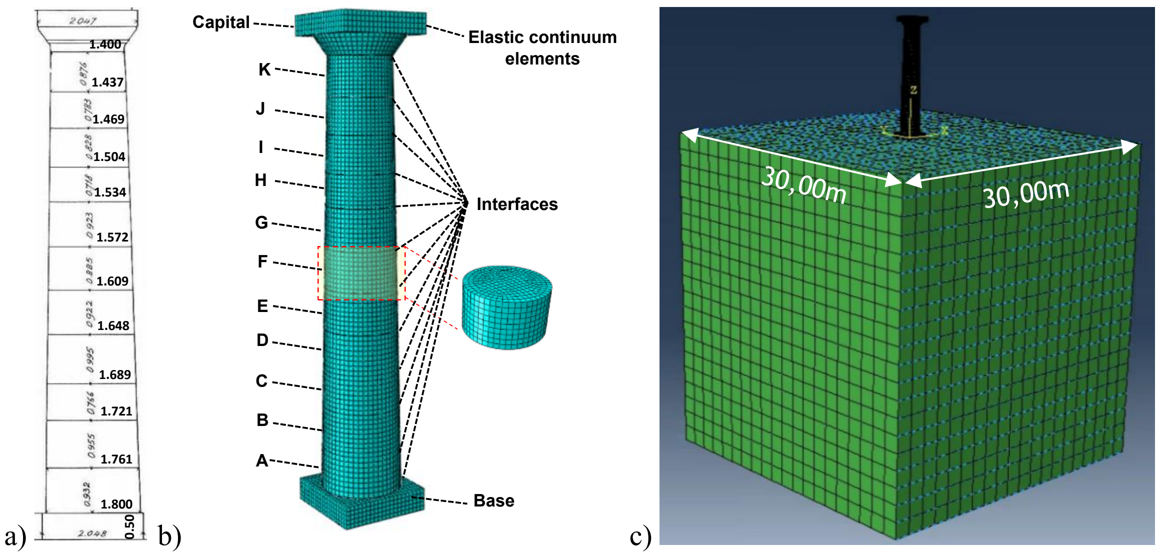

Figure 1. *a) Geometric properties of the column (all dimensions are given in metres), b) Numerical model of the column at the Parthenon of the Acropolis of Athens and c) 3D SSI numerical model*

All components are assigned the mechanical properties of Pentelic marble (modulus of elasticity E = 45.0 GPa, Poisson's ratio v = 0.33 and density ρ = 2.7 t/m³) and are assumed linear elastic. Material nonlinearity is not considered; all nonlinear response arises from geometric effects and contact interactions. Inter-drum interfaces and the interface between the lowest drum and the stylobate are modelled using a finite-sliding hard-contact formulation that prevents penetration in compression and allows full detachment under uplift. Tangential behaviour follows a Coulomb friction model with friction coefficient μ = 0.7, consistent with experimental evidence and commonly used in the literature (Papantonopoulos et al., 2002; Komodromos et al., 2008). No artificial bonding or additional kinematic constraints are introduced. Damping is not assigned to the structural components, as even small viscous damping may unrealistically suppress rocking amplitudes during strong shaking (Papantonopoulos et al., 2002; Psycharis, 2014).

The column is analysed both in a deformable-soil configuration and in a rigid-base reference configuration, representing EC8 Soil Class A conditions. In the latter case, the base of the lowest drum is fully constrained, providing a benchmark to isolate pure soil–structure interaction effects and to quantify the influence of soil deformability on rocking stability.

Soil Modelling and Boundary Conditions

The soil domain is modelled as a fully three-dimensional deformable continuum, in which the finite near-field soil is coupled to an equivalent semi-infinite elastic half-space through free-field kinematic lateral boundaries and Lysmer–Kuhlemeyer dashpots at the base. The near-field soil beneath and around the column is discretised using solid elements with elasto-plastic Mohr–Coulomb behaviour, with plastic yielding enabled in all soil profiles throughout the analyses, while radiation damping and far-field energy dissipation are reproduced through dashpot-based absorbing boundaries. A soil depth of 30 m is adopted, consistent with current code provisions, which classify site conditions on the basis of an equivalent shear-wave velocity for the upper 30 m ($V_{S,30}$), assuming uniform properties with depth within the soil domain. This idealisation allows the influence of soil stiffness on SSI and rocking behaviour to be isolated without introducing additional complexity due to stratification. The soil domain extends 30 m in width and 30 m in length, centred below the column, resulting in a 30 × 30 × 30 m deformable block (Figure 1c). This domain is sufficiently large to accommodate the deformation field associated with foundation rocking and SSI.

To investigate the role of local site conditions and the effects of SSI, three single-layer sand profiles corresponding to EC8 Soil Classes B, C and D are analysed, while a fixed-base (bedrock) configuration is used to represent rigid Class A. Their density, shear-wave velocity, bulk modulus and friction angle are drawn from the calibrated soil sets provided in D. Pitilakis & Petridis (2022). Table 1 reports these fundamental geotechnical properties, which constitute the reference input data for the present study. This ensures physically compatible combinations of stiffness and strength parameters and allows direct comparison of soil–structure interaction effects across different stiffness levels. The small-strain shear modulus is calculated as:

$$G = \rho V_s^2 \tag{1}$$

where ρ is the soil mass density and V_s is the shear-wave velocity. The remaining elastic constants are then derived from the bulk modulus K and the calculated G using standard isotropic elasticity relations.

The soil behaviour is simulated using an elasto-plastic Mohr–Coulomb model, which is well suited for drained, predominantly frictional granular deposits typically underlying ancient temples. All analyses are performed under drained conditions, neglecting excess pore pressure generation, which is considered reasonable for the examined soil types and the scope of the study. For all sand profiles, a small apparent cohesion of c = 1 kPa is adopted, reflecting possible light cementation and ageing of shallow deposits and providing numerical regularisation without artificially increasing shear strength. This value remains low relative to the frictional resistance and is consistent with cohesion levels commonly assumed in similar SSI studies (e.g. Tubaldi et al., 2015). The plastic response is governed by the friction angle assigned to each soil class, and a small dilation angle $\psi = 3°$ is adopted for all sand profiles.

Material damping is introduced through Rayleigh coefficients calibrated to approximately 2% equivalent damping around the predominant period of each soil profile. The coefficients α and β are obtained by matching ξ = 2% at the fundamental soil period $T_1 = 4H/V_s$ and at a second period $T_2 = T_1/3$ (corresponding to $\omega_2 = 3\omega_1$), ensuring appropriate damping control over both low- and high-frequency components of the seismic response. Table 2 reports the resulting Rayleigh coefficients together with the derived elastic constants G, E, ν used in the Abaqus elastic material definitions associated with the Mohr–Coulomb soil model. The elastic constants are computed using the standard isotropic elasticity relations:

$$E = \frac{9KG}{3K+G} \tag{2}$$

$$\nu = \frac{3K-2G}{2(3K+G)} \tag{3}$$

where E is Young's modulus, ν is Poisson's ratio, K is the bulk modulus and G is the shear modulus, ensuring full consistency between the geotechnical input of Table 1 and the numerical model.

Table 1. *Soil parameter values used along with chosen soil types according to EC8, adopted from D. Pitilakis & Petridis (2022)*

Parameters	**Sand**		
	Loose	**Medium**	**Med-dense**
Soil mass density, ρ [Mg/m^3]	1.7	1.9	2.0
Bulk modulus, K [kPa]	1.5×10^5	2.0×10^5	3.0×10^5
Cohesion, c [kPa]	1.0	1.0	1.0
Shear strain at max shear	0.1	0.1	0.1
Friction angle, φ [deg]	29.0	33.0	37.0
Shear-wave velocity, Vs [m/s]	150	300	450
Type (EC8)	D	C	B

The finite soil domain is truncated laterally using kinematic constraints that enforce free-field conditions and prevent spurious boundary reflections during seismic loading. Specifically, nodes located on opposite vertical boundaries of the soil domain are paired at the same elevation and connected through multi-point constraints (MPCs), enforcing identical translational displacements in the horizontal directions. This approach is equivalent to periodic (free-field) boundary conditions commonly adopted in nonlinear site response and SSI analyses, allowing vertically propagating shear waves to pass through the boundaries without artificial reflection while preserving realistic shear deformation within the soil mass (Joyner & Chen, 1975; Wolf, 1985). No fixed translational restraints are imposed at the lateral boundaries, ensuring that soil plasticity and strain localisation can develop naturally during strong ground motion.

Table 2. *Derived elastic constants, Rayleigh damping coefficients and characteristic periods of the sand profiles used in the Abaqus SSI analyses*

Soil Profile (EC8)	**G=ρVs² (kPa)**	**E (kPa)**	**ν (-)**	**ψ dilation (deg)**	**T1 (s)**	**α (1/s)**	**β (s)**
Sand – Loose (D)	38,250	105,760	0.382	3	0.800	0.2356	0.001273
Sand – Medium (C)	171,000	399,222	0.167	3	0.400	0.4712	0.000637
Sand – Med-dense (B)	405,000	837,931	0.034	3	0.267	0.7069	0.000424

At the base of the soil domain, the finite rigidity of the underlying bedrock is represented through Lysmer–Kuhlemeyer viscous dashpots, simulating radiation damping into a semi-infinite elastic half-space (Lysmer & Kuhlemeyer, 1969). A layer of auxiliary bedrock nodes is introduced below the soil base and connected to the corresponding soil nodes through dashpot elements. The underlying elastic bedrock half-space is characterised by a shear-wave velocity of 800 m/s and a mass density of 2.2 Mg/m³. The seismic excitation is applied at the soil–dashpot interface (soil base), while the dashpot base nodes are fully fixed, allowing incident waves to propagate upward into the soil and outgoing waves to be absorbed by the dashpots without spurious reflection.

This modelling strategy ensures a realistic representation of the deformable ground, enabling the simulation to capture soil deformability, radiation damping and potential plastic yielding, together with the full suite of nonlinear SSI mechanisms that influence the rocking stability of ancient multi-drum columns.

Soil–Structure Interaction and Dynamic Analysis Setup

Soil–structure interaction is primarily governed by the dynamic response and deformability of the supporting soil, which control the modification of the input motion, radiation damping and foundation compliance. Within this framework, the column–soil interface is modelled using frictional surface-to-surface contact, enabling sliding, uplift, separation and re-contact to develop naturally during seismic excitation. No artificial restraints or bonding are introduced at the base of the column, ensuring that all resisting forces arise solely from the stiffness, strength and inertial properties of the underlying soil. The fixed-base configuration (Class A) is modelled by fully constraining the base of the column, eliminating compliance and radiation damping effects and thereby providing a reference for assessing SSI influence. The soil–column interface employs the same Coulomb friction law (μ=0.7) as that applied between the drums.

The analyses are performed in two steps, with geometric nonlinearities activated in both steps to capture potential uplift, large rotations and second-order effects. The first step is a quasi-static gravity analysis, which establishes the initial stress state in the soil and stabilises the contact forces between all drums and between the column and the ground. The second step consists of a fully dynamic implicit time-history analysis, where the seismic action is applied and the full nonlinear rocking–sliding behaviour develops. Automatic time incrementation is employed to ensure convergence during phases of intense contact activity and high-frequency impact events.

Since the seismic response of rocking systems is highly sensitive to the frequency content of the input motion, careful selection and scaling of earthquake records is essential. To assess the potential influence of spectral characteristics and SSI on the rocking response, two real earthquake records with contrasting frequency content are employed: the Kefalonia M_w 6.2 earthquake record (26.01.2014), representative of strong, high-frequency shaking in western Greece, and the Takatori record from the 1995 Kobe M_w 6.9 earthquake, exhibiting stronger long-period components. Both records are scaled to PGA values of 0.25g and 0.81g, corresponding respectively to a design-level event (10% probability of exceedance in 50 years) and to an extreme seismic scenario (1% probability of exceedance in 50 years). The acceleration time histories and normalised 5%-damped acceleration response spectra of the selected ground motions are presented in Figure 2.

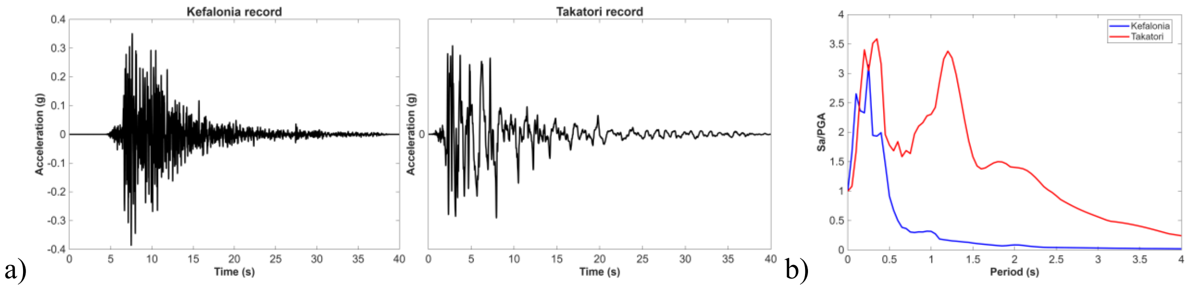

Figure 2. *a) Acceleration time histories and b) normalised response spectra for the selected real records (Kefalonia M_w 6.2 record and Takatori record from Kobe M_w 6.9 1995 event)*

The seismic excitation is imposed as a prescribed horizontal acceleration time history at the soil–dashpot interface, ensuring compatibility with the absorbing boundary formulation and a physically consistent input of the incoming wavefield. Only uniaxial (x) horizontal excitation is considered, while vertical ground motion is neglected, in line with common practice for rocking-dominated systems, because rocking and sliding of multi-drum columns are primarily governed by horizontal inertia forces. Through the Lysmer–Kuhlemeyer dashpots, the incident waves propagate into the soil while energy is simultaneously radiated back into the underlying half-space, providing a realistic representation of seismic bedrock excitation in the presence of soil–structure interaction.

RESULTS AND DISCUSSION

The seismic response of the free-standing multi-drum column is quantified using four complementary engineering demand parameters (EDPs), combining traditional global measures with cycle-based kinematic indices that are better aligned with the physical response of rocking systems on deformable foundations. Two global EDPs are first evaluated from the capital displacement history, namely the peak normalised top displacement:

$$u_{\text{top}} = \frac{\max|u_{\text{cap}}(t)|}{D_{\text{base}}} \tag{4}$$

and the residual normalised top displacement:

$$u_{\text{res,top}} = \frac{|u_{\text{cap,res}}|}{H} \tag{5}$$

where $u_{\text{cap}}(t)$ is the horizontal displacement of the capital, $u_{\text{cap,res}}$ is its permanent value at the end of shaking, D_{base} is the base diameter of the lowest drum and H is the total column height. These indices provide an overall measure of transient rocking demand and permanent tilt (loss of re-centring), respectively, and are summarised versus the input PGA values in Figure 3.

Figure 3 demonstrates that the introduction of SSI substantially alters both the peak and residual response compared to the fixed-base configuration; however, the influence of soil stiffness is neither proportional nor strictly monotonic across all excitation levels and ground motions. To facilitate an easy reading of the figure, the vertical axis is truncated at $u_{\text{top}} = 1$ and $u_{\text{res,top}} = 2.0\%$. Beyond these limits, the numerical analyses indicate toppling of the capital or total collapse of the column; such cases are denoted by the symbol ∞ in the figure. A key observation is that neither u_{top} nor $u_{\text{res,top}}$ increases systematically from Soil Class B to C and D. The compiled numerical values show that, under strong Takatori excitation (PGA = 0.81 g), the softest soil (Class D) does not necessarily exhibit the largest residual displacement and may develop values comparable to or smaller than those of the fixed-base or intermediate-soil cases. These observations indicate that soil compliance introduces competing mechanisms: while reduced stiffness enhances foundation deformability and rocking propensity, it also modifies the effective input motion and increases radiation damping, such that the resulting response depends on the combined interaction of soil flexibility, rocking asymmetry and ground-motion characteristics rather than on stiffness alone.

This behaviour further suggests that global displacement-based indices, although appropriate for fixed-base configurations, may not be fully representative of the response when the foundation is deformable. In SSI cases, part of the measured capital displacement reflects foundation motion and soil compliance rather than purely the rocking kinematics of the column itself. Consequently, peak and residual top displacements may mask important differences in cycle development and drift accumulation that occur at the base interface. This limitation motivates the introduction of cycle-based kinematic EDPs that more directly capture the mechanics of rocking on deformable soil.

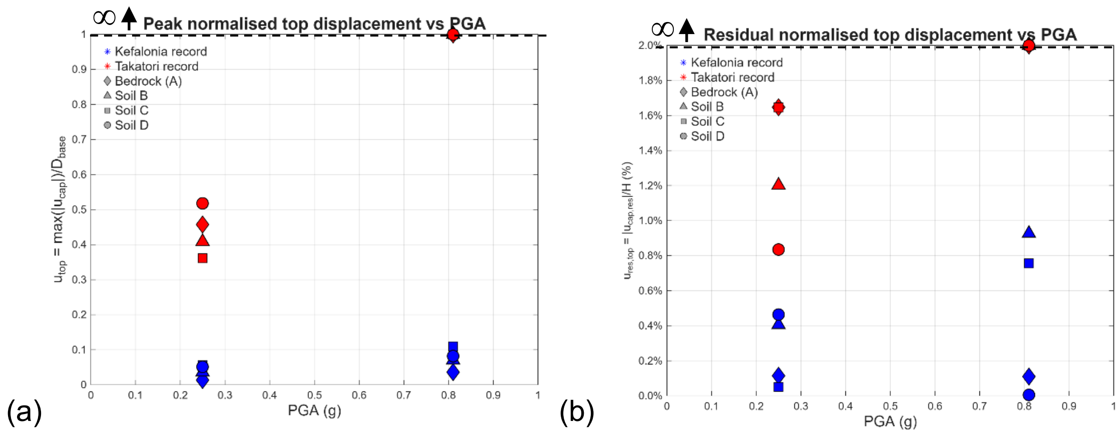

Figure 3. (a) *Normalised maximum capital displacement, u_{top} =max(u_{cap})/D_{base}, and (b) residual normalised capital displacement $\boldsymbol{u_{res,top}}$ =| $\boldsymbol{u_{cap,res}}$ |/$\boldsymbol{H}$ versus PGA for the fixed-base and SSI cases (Soil Classes B, C, D) under the selected ground motions*

To better capture the cyclic rocking kinematics and the progressive accumulation of permanent offsets, additional cycle-based EDPs are derived from the horizontal displacement histories $U_1(t)$ at two opposite points at the base of the first drum. An equivalent base rotation time history is computed as:

$$\theta(t) = \frac{U_1^{(+)}(t) - U_1^{(-)}(t)}{L} \tag{6}$$

where $U_1^{(+)}(t)$ and $U_1^{(-)}(t)$ are the displacements at opposite base points and L is their distance, equal to the diameter of the first drum. Individual rocking cycles k are identified from successive positive and negative extrema of $\theta(t)$. For each cycle, the peak-to-peak rocking amplitude is defined as:

$$A_k = \theta_k^+ - \theta_k^- \tag{7}$$

while the cycle midpoint (drift) is defined as:

$$m_k = \frac{\theta_k^+ + \theta_k^-}{2} \tag{8}$$

In addition, a loss-of-recentring ratio per cycle is introduced as:

$$R_k = \frac{|m_k|}{A_k} \tag{9}$$

providing a dimensionless measure of cycle asymmetry and progressive bias away from zero rotation.

Figure 4 summarises the cycle-based response through two scalar measures extracted from these sequences: (a) the maximum cyclic amplitude, $A_{\max} = \max_k A_k$, and (b) the maximum absolute cycle drift, $\max \mid m_k \mid$, plotted versus PGA. Compared to the previous global displacement-based EDPs, these measures provide clearer insight into SSI-driven mechanisms. While $A_{\max}$ reflects the intensity of bidirectional rocking oscillations, $\max m_k$ directly quantifies the accumulation of permanent rotation associated with asymmetric cycles and soil yielding. It should be noted that, in contrast to Figure 3, collapse cases are not explicitly represented in Figure 4, as cycle-based quantities cannot be meaningfully defined once overturning or loss of stability occurs. Therefore, the ∞ symbols used in Figure 3 to denote collapse are not included in the cycle-based representation.

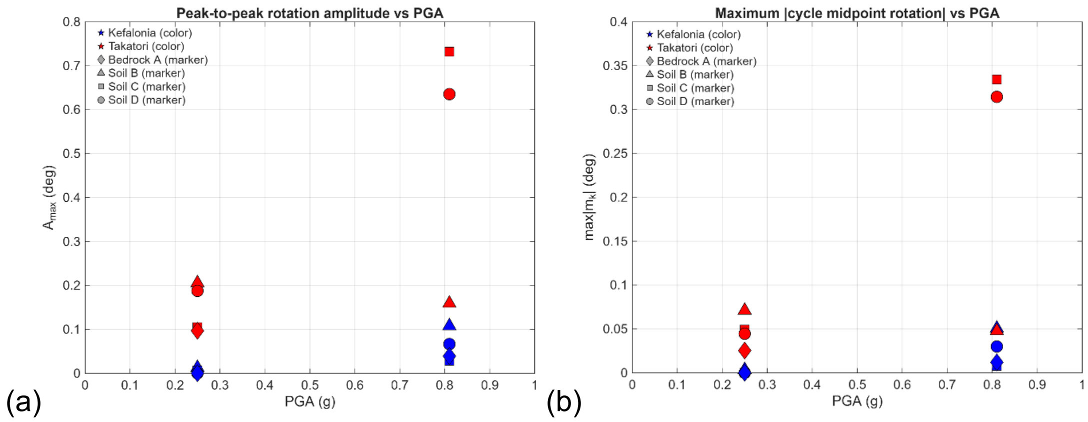

Figure 4. *(a) Cycle-based peak-to-peak rotation amplitude summary measure ($\boldsymbol{A_{max}}$) and (b) cycle-based drift summary measure ($\boldsymbol{max} \mid \boldsymbol{m_k} \mid$) versus PGA for the fixed-base (Class A) and SSI cases, computed from U1 histories at opposite points at the base of the first drum*

A clearer differentiation between soil classes emerges when examining $\max \mid m_k \mid$ rather than the residual global index $u_{\text{res,top}}$, indicating that cycle asymmetry captures soil-induced mechanisms more explicitly than top displacement alone. Even in cases where residual capital displacement remains comparable across soils, the cycle-based drift measure reveals differences in the internal rocking mechanism and in the degree of asymmetry induced by foundation deformability. This confirms that permanent deformation accumulation in SSI systems is governed primarily by cycle imbalance rather than by peak displacement alone. A clear difference also emerges between the two ground motions. Under the Takatori record, a larger number of well-defined rocking cycles develop, leading to higher values of both $A_{\max}$ and $\max \mid m_k \mid$, whereas under the Kefalonia record the response is often characterised by fewer cycles and, in several cases, by rotations remaining below the adopted detection threshold. Thus, for the Kefalonia record some analyses exhibit negligible cycle-based demand, not because SSI is absent, but because the rocking response does not reach amplitudes sufficient to trigger sustained cyclic motion within the selected kinematic threshold. This highlights the strong role of ground-motion frequency content and duration in governing cycle development and drift accumulation. The physical origin of these trends is further illustrated in Figures 5 and 6, which indicatively present representative time histories of rotation $\theta(t)$ and the corresponding evolution of A_k, m_k and R_k for Takatori and Kefalonia cases on Soil Class D.

For the long-period–rich Takatori record (Figure 5), the rotation history exhibits sustained bidirectional oscillations with progressively increasing bias, leading to monotonic growth of m_k and elevated values of R_k. The gradual shift of cycle midpoints away from zero indicates incomplete re-centring after each oscillation and reflects the cumulative effect of soil deformability and asymmetric contact conditions at the drum interface. In contrast, the predominantly high-frequency Kefalonia record (Figure 6) shows fewer pronounced cycles and smaller drift accumulation, with m_k fluctuating closer to zero and lower R_k values. Although peak rotations may occur, the absence of sustained asymmetric cycles limits the development of permanent rotation. This comparison demonstrates that deformation accumulation is controlled more by the sequence and symmetry of rocking cycles than by isolated peak values, while the frequency content of the input ground motion also plays an important role.

Overall, the results indicate that foundation soil effects on the seismic response of free-standing multi-drum columns are significant but not proportional to soil stiffness alone. While global EDPs such as u_{top} and $u_{\text{res,top}}$ remain useful for describing overall instability and ultimate performance limits, cycle-based drift measures (A_k, $\max |m_k|$ and R_k) are essential for capturing the underlying rocking kinematics and the accumulation of irreversible deformation under SSI conditions, particularly when the foundation is not effectively rigid. This combined interpretation reconciles the apparent ambiguities observed in the global indices and provides a physically consistent framework for understanding how soil deformability modifies the stability and post-earthquake performance of multi-drum columns.

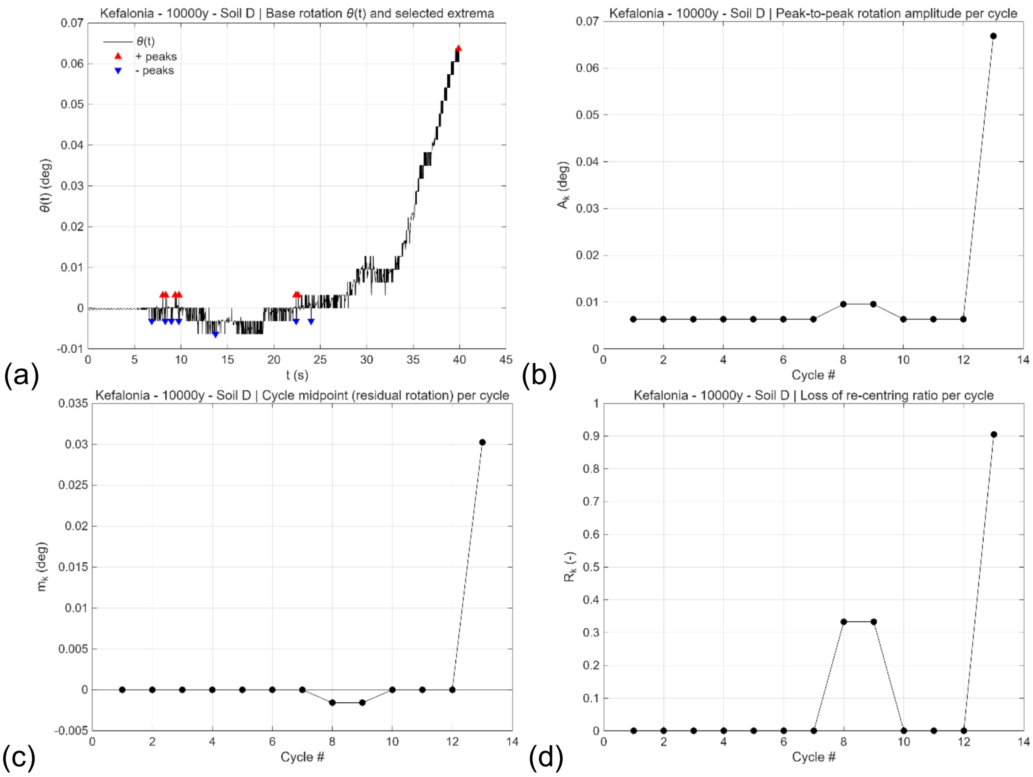

Figure 5. *Representative cycle-by-cycle response for Kefalonia record scaled to 0.81g for the SSI case - Soil Class D: (a) base rotation time history $\boldsymbol{\theta(t)}$ and identified extrema used to define cycles, (b) peak-to-peak rotation amplitude per cycle $\boldsymbol{A_k}$, (c) cycle mid-point (drift) per cycle $\boldsymbol{m_k}$, and (d) loss-of-recentring ratio per cycle $\boldsymbol{R_k}$, derived from U1 at opposite points at the base of the first drum*

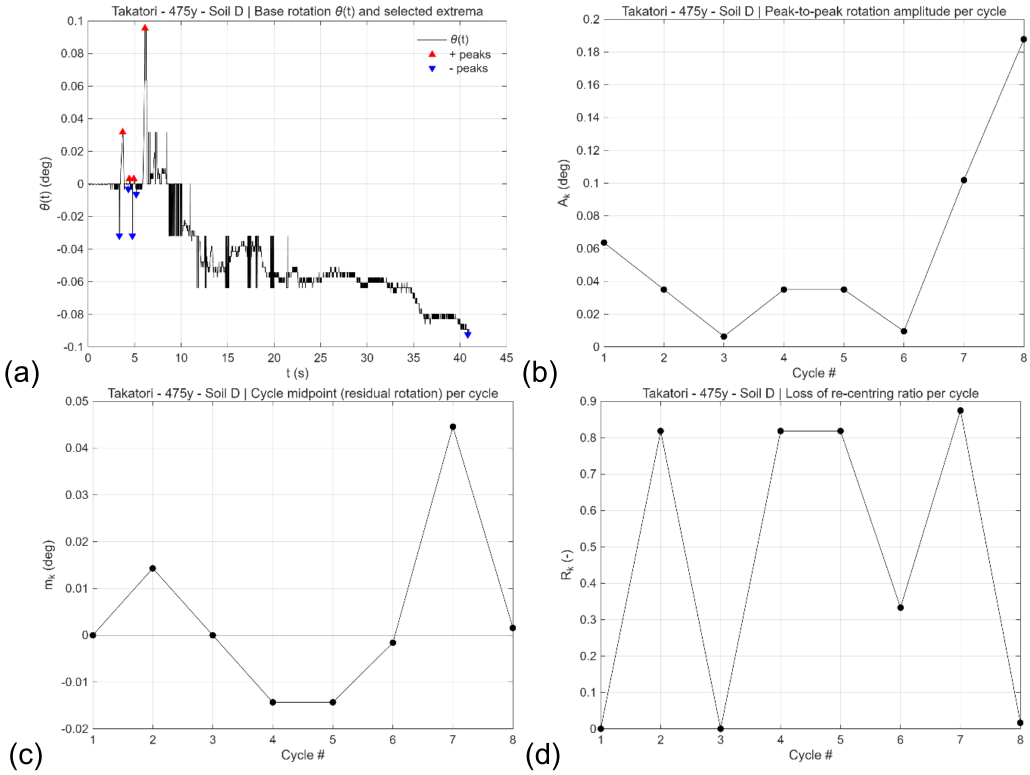

Figure 6. *Representative cycle-by-cycle response for Takatori record scaled to 0.25g for the SSI case - Soil Class D: (a) base rotation time history $\boldsymbol{\theta(t)}$ and identified extrema used to define cycles, (b) peak-to-peak rotation amplitude per cycle $\boldsymbol{A_k}$, (c) cycle mid-point (drift) per cycle $\boldsymbol{m_k}$, and (d) loss-of-recentring ratio per cycle $\boldsymbol{R_k}$, derived from U1 at opposite points at the base of the first drum*

CONCLUSIONS

This study represents a first comprehensive effort to investigate the seismic response of a free-standing multi-drum column by explicitly accounting for soil–structure interaction effects associated with different foundation conditions. A fixed-base configuration representing bedrock conditions was compared with three deformable sand profiles corresponding to Eurocode 8 soil classes B, C and D, using fully nonlinear three-dimensional dynamic analyses. The results demonstrate that the influence of soil deformability on the column response is significant and governed by interacting and combined nonlinear mechanisms. While softer soils generally modify and, in several cases, amplify the deformation demand, the response does not scale proportionally with decreasing soil stiffness across all excitation levels and all engineering demand parameters. In particular, global peak and residual displacement EDPs, although useful for describing overall instability and permanent tilt, are not sufficient on their own to capture the complex rocking kinematics that develop when the base of the column is no longer effectively fixed. Local soil compliance, foundation rotation and radiation damping, all affected by the frequency content of the input motion, alter both the amplitude and the temporal evolution of the response, introducing competing mechanisms that cannot be interpreted solely through single scalar measures.

A clearer insight into the role of soil–foundation multi-drum column interaction is obtained by examining cycle-based and relative-motion EDPs, which explicitly describe the evolution of bidirectional oscillations, cumulative drift and loss of re-centring capacity. These measures reveal that soil conditions primarily affect the persistence and accumulation of deformation rather than only the maximum instantaneous demand, thus highlighting that the governing mechanism under SSI is progressive kinematic bias rather than merely amplified peak rotation. The comparative response under different ground motions further indicates that the interaction between soil properties and excitation characteristics plays a key role in controlling the observed response, particularly for long-duration or low-frequency records, where the number and asymmetry of rocking cycles become critical for permanent deformation accumulation.

Overall, the findings confirm that SSI is a governing factor in the seismic behaviour of ancient multi-drum columns resting on deformable soils and cannot be adequately represented through rigid-base assumptions or single scalar EDPs. The results support the need for kinematically informed demand measures that capture both absolute and relative displacements along the height of the column, providing a more physically consistent basis for seismic assessment, interpretation of observed damage, and future conservation-oriented analyses.

ACKNOWLEDGEMENTS

The authors sincerely thank Ms Vasiliki Eleftheriou, director of the Acropolis Restoration Service in Athens (YSMA), for providing all the relevant data for the case study.

REFERENCES

Amendola, C., & Pitilakis, D. (2022). Vulnerability assessment of historical cities including SSI and site effects. Geotechnical Engineering for the Preservation of Monuments and Historic Sites III, Lancellotta, Viggiani, Flora, de Silva & Mele (Eds), Taylor & Francis Group, https://doi.org/10.1201/9781003308867.

Dassault Systèmes. (2022). Abaqus 2022 Documentation. Dassault Systèmes SIMULIA Inc., Providence, RI, USA.

Joyner, W. B., & Chen, A. T. F. (1975). Calculation of nonlinear ground response in earthquakes. Bulletin of the Seismological Society of America, 65(5), 1315–1336.

Karatzetzou, A., Pitilakis, D., & Karafagka, S. (2021). System Identification of Mosques Resting on Soft Soil. The Case of the Suleiman Mosque in the Medieval City of Rhodes, Greece. Geosciences, 11(7), 275.

Komodromos P, Papaloizou L, Polycarpou P (2008) Simulation of the response of ancient columns under harmonic and earthquake excitations. Engineering Structures, 30(8), 2154–2164.

Konstantinidis, D., & Makris, N. (2005). Seismic response analysis of multi-drum classical columns. Earthquake Engineering & Structural Dynamics, 34(10), 1243-1270.

Lysmer, J., & Kuhlemeyer, R. L. (1969). Finite dynamic model for infinite media. Journal of the Engineering Mechanics Division, ASCE, 95(EM4), 859–877.

Marinos, V., Prountzopoulos, G., Papouli, D., Michalopoulou, D., & Eleftheriou, V. (2025). Geotechnical Assessment of Foundation Stability for Preserving the Agrippa Monument at the Acropolis of Athens. Sensors, 25, 219.

Papantonopoulos, C., Psycharis, I.N., Papastamatiou, D.Y., et al. (2002) Numerical prediction of the earthquake response of classical columns using the distinct element method. Earthq Eng Struct Dyn, 31(9), 1699-1717.

Pitilakis, D. & Petridis, C. (2022). Fragility curves for existing reinforced concrete buildings, including soil-structure interaction and site amplification effects. Eng. Struct., 269, 114733, DOI:10.1016/j.engstruct.2022.114733.

Pitilakis, K., Tsinidis, G., Karafagka, S. (2017). Analysis of the seismic behaviour of classical multi-drum and monolithic columns, Bulletin of Earthquake Engineering, 15, 5281-5307, DOI: 10.1007/s10518-017-0160-4.

Psycharis, I.N. (2014). Ancient monuments under seismic actions: modelling and analysis. In: Beer, M., Kougioumtzoglou, I., Patelli, E., Au I S-K A (eds) Encyclopaedia of Earthquake Engineering, Springer Berlin Heidelberg. doi: 10.1007/978-3-642-36197-5_145-1.

Stiros, S.C. (2020). Monumental articulated ancient Greek and Roman columns and temples and earthquakes: archaeological, historical, and engineering approaches. Journal of Seismology, 24, 853–881.

Thompson, H. (1953). Excavations in the Athenian Agora: 1953. Hesperia 23, 31–67.

Tsatsanifos, C. (2023). Preservation and restoration of monuments: The authenticity principle in geotechnical interventions. Smart Geotechnics for Smart Societies, Zhussupbekov, Sarsembayeva & Kaliakin (Eds), Taylor & Francis Group, ISBN 978-1-003-29912-7.

Tubaldi, E., Antonopoulos, C., Mitoulis, S.A. et al. (2023). Field tests and numerical analysis of the effects of scour on a full-scale soil–foundation–structural system. Journal of Civil Structural Health Monitoring, 13, 1461–1481.

Wolf, J. P. (1985). Dynamic Soil–Structure Interaction. Prentice-Hall, Englewood Cliffs, NJ.